ACS APPLIED MATERIALS & INTERFACES

Research Article

www.acsami.org

Improved Cell Adhesion and Osteogenesis of op-HA/PLGA Composite by Poly(dopamine)-Assisted Immobilization of Collagen Mimetic Peptide and Osteogenic Growth Peptide

Zongliang Wang,[†] Li Chen,[‡] Yu Wang,[†] Xuesi Chen,[†] and Peibiao Zhang*[,†]

[†]Key Laboratory of Polymer Ecomaterials, Changchun Institute of Applied Chemistry, Chinese Academy of Sciences, Changchun 130022, PR China

[‡]School of Pharmaceutical Sciences, Jilin University, Changchun 130021, PR China

Supporting Information

ABSTRACT: A nanocomposite of poly(lactide-*co*-glycolide) (PLGA) and hydroxyapatite (HA) with a different grafting ratio of L-lactic acid oligomer (op-HA) showed better interface compatibility, mineralization, and osteogenetic abilities. However, surface modification of the composite is crucial to improve the osteointegration for bone regeneration. In this study, a biomimetic process via poly(dopamine) coating was utilized to prepare functional substrate surfaces with immobilized bioactive peptides that efficiently regulate the osteogenic differentiation of preosteoblasts (MC3T3-E1). Our study demonstrated that incorporation of collagen mimetic peptide significantly enhanced cell adhesion and proliferation. The immobilization of osteogenic growth peptide induced the osteodifferentiation of cells, as indicated by the alkaline phosphate activity test, quantitative real-time polymerase chain reaction analysis, and immunofluorescence staining. The mineralization on the peptide-modified substrates was also enhanced greatly. Findings from this study revealed that this biofunctionalized layer on op-HA/PLGA substrate improved mineralization and osteogenic differentiation. In conclusion, the surface modification strategy with bioactive peptides shows potential to enhance the osteointegration of bone implants.

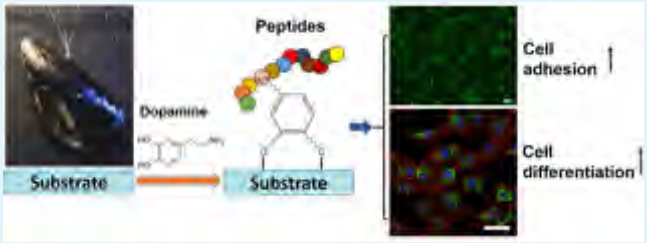

KEYWORDS: *collagen mimetic peptide, osteogenic growth peptide, composite, adhesion, osteogenesis, dopamine*

1. INTRODUCTION

Bone tissue engineering shows great potential in developing novel biomaterials as bone substitutes and grafts for bone regeneration therapies.[1,2] Hydroxyapatite (HA) is a promising biomaterial used in bone substitute, as it is a normal constituent of bone. HA has the particular ability to bind directly to bone.[3] However, the major limitations of the use of HA ceramic are its mechanical properties, owing to its brittleness and poor fatigue resistance.[4] Composites of poly(lactide-*co*-glycolide) (PLGA) and HA have been developed into orthopedical materials.[5,6] In our previous study, hydroxyapatite nanoparticles (n-HA) with different grafting ratios of L-lactic acid oligomer (op-HA) were synthesized without any catalyst. The dispersion of op-HA nanoparticles was better than n-HA either in chloroform or nanocomposites. It was found that the op-HA/PLGA composites with an appropriate grafting ratio of L-lactic acid oligomer exhibited better mineral deposition, strong biomineralization, and osteogenesis abilities in vitro and in vivo.[7] However, surface modification of implants to improve biological performance, such as promoting cell growth and differentiation, would be critical for developing functional bone and dental materials.

Surface modification of composites or scaffolds using cell-adhesive peptides, osteoinductive growth factors, or other molecules could compensate for the lack of osteointegration of the substrates.[8−11] Growth factor proteins, such as BMP-2, are easily degraded by proteinases in human body. Overabundant BMP-2 might lead to side effects, such as heterotopic osteogenesis, immunoreaction, and tumorigenesis.[12] Approaches using small compounds, especially peptides, could be beneficial compared with growth factors due to less expense and a more steady, easy accessibility.[13] For instance, RGD peptides have been applied more commonly to improve cell adhesion and proliferation in bone tissue engineering.[14,15] However, some studies revealed that RGD was detrimental to MSC attachment.[16,17] Collagen-derived peptides might be an alternative to RGD for functionalization of materials with osteogenic cell attachment.[18] One of the collagen mimetic peptides, P15 (GTPGPQGIAGQRGVV), is characterized as the domain for cell-binding of human collagen type I protein.[19] It was reported that P15 peptide could promote adhesion, proliferation, and differentiation of osteoblasts.[20,21] A higher rate of cell proliferation appeared on biologically inert grafting materials coating by P15 (PepGen P-15, Dentsply FRIADENT,

Received: July 16, 2016
Accepted: September 21, 2016
Published: September 21, 2016

DOI: 10.1021/acsami.6b08733
ACS Appl. Mater. Interfaces 2016, 8, 26559−26569

Scheme 1. Schematic Illustration of Dopamine-Assisted Immobilization of Collagen Mimetic Peptide and Osteogenic Growth Peptide on op-HA/PLGA Composite Substrate[a]

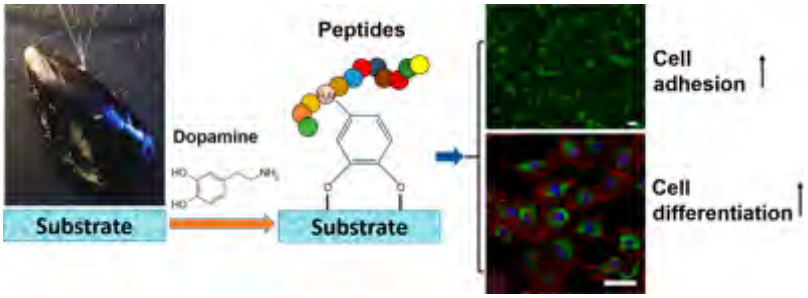

[a]The photograph of a mussel attached on the substrate was reprinted by permission from Macmillan Publishers Ltd: Nature,[38] copyright (2007).

Mannheim, Germany), and accelerated formation of highly vascularized bone was also obtained.[22] In addition, different types of osteoinductive peptides have been exploited.[23] Osteogenic growth peptide (OGP) is a naturally occurring peptide (ALKRQGRTLYGFGG) in bone marrow, with an active OGP (10−14) fragment being proved to directly regulate hMSC osteoblast differentiation.[24−26] OGP has been applied to monitor osteoblasts proliferation, differentiation, and mineralization in vitro.[8,9,27] Furthermore, OGP promotes endochondral bone formation in rats and rabbits, thereby enhance fracture healing in vivo.[28−31]

A poly(dopamine) (pDA) deposition process for incorporation of peptides or growth factors on titanium implants or porous scaffolds has also been utilized to potentiate the regenerative capacity of cells for bone regeneration in vitro and in vivo.[14,32−34] The pDA-assisted immobilization strategy was inspired by mussel-adhesion phenomena in nature.[35] Under alkaline conditions, oxidation of the catechol groups forms a poly(dopamine) layer on various materials, such as polymers and metals.[14] It may offer a simple and effective platform to immobilize peptides and proteins onto the polymeric scaffolds.[33,34,36] Li et al. found that biomimetic hybridized polydopamine/calcium phosphate apatite grafts could dramatically enhance in vivo osseointegration.[1] Poly(dopamine) (pDA) was utilized as template to synthesize nano-HA, which was subsequently incorporated into polycaprolactone using a coelectrospinning method. The prepared nanofiber scaffold exhibited enhanced cytocompatibility and osteogenic capacity.[37] Poly(dopamine)-assisted immobilization of RGD, HA, and BMP-2 also promoted osteogenic differentiation of MSC and mineralization.[14]

Thus, in this study, we report pDA-assisted immobilization of collagen mimetic peptide (P15) and osteogenic growth peptide (OGP) onto op-HA/PLGA substrate to enhance the cell adhesion and osteogenic differentiation of mouse preosteoblasts (MC3T3-E1) in vitro, as shown in Scheme 1.[38,39] The aim of this study was to improve cell affinity and osteoinduction ability of composite surfaces with immobilization of P15 and OGP peptides via the poly(dopamine)-coating process. The adhesion, proliferation, and osteodifferentiation of MC3T3-E1 cells were explored to investigate the effectiveness of the surface modification with peptides.

2. EXPERIMENTAL SECTION

2.1. Materials. L-Lactide and glycolide were supplied by Purac. The chemicals were offered by Sigma-Aldrich. The grade of chemicals was analytical grade or higher. HA powder was obtained from Nanjing Emperor Nano Material Co., Ltd. Collagen mimetic peptide (GTPGPQGIAGQRGVV, abbreviated as P15) and osteogenic growth peptide (ALKRQGRTLYGFGG, abbreviated as OGP) were purchased from GL Biochem (Shanghai) Co., Ltd.

2.2. Synthesis of Polymer. PLGA was synthesized in our lab according to the literature procedure (see the Supporting Information).[40] The average molecular weight was about 86 000 and the ratio of LA:GA was 80:20.

2.3. Preparation of op-HA. L-Lactic acid oligomer was grafted onto HA surface by formation of a Ca−carboxylate bond without catalyst according to our previous work (see the Supporting Information), and the prepared op-HA was vacuum-dried.[41]

2.4. Preparation of Composite. The op-HA powder was evenly dispersed in chloroform. Afterward, the suspension was transferred into a 6% (w/v) PLGA/chloroform solution to achieve an op-HA content of 20 wt % in the composite. Then ∼30 μL of the composite solution was coated onto a cover slide with a side length of 24 mm preliminary treated with 2% dimethyldichlorosilane (DMDC, Fluka). The op-HA/PLGA-coated slides were vacuum-dried for 48 h under ambient temperature and sterilized by UV radiation for 30 min prior to use.

2.5. pDA-Assisted Immobilization of Peptides onto op-HA/PLGA Composite. The pDA-coating process was carried out according to the literature procedure.[42] The op-HA/PLGA composites were soaked in dopamine solution (2 mg/mL in 10 mM Tris·HCl, pH 8.0) and put on an oscillator for 2 h under ambient temperature (pDA/op-HA/PLGA). The pDA-coated composites were washed with deionized water five times to remove free dopamine. Afterward, P15 (2 mg/mL in PBS) and OGP (0.1 mg/mL in PBS) were introduced on pDA/op-HA/PLGA or op-HA/PLGA composites for another 2 h. The composites were gently washed with deionized water three times to remove the free peptides. The compositions of unmodified and modified substrates are listed in Table 1.

Table 1. Compositions of Poly(dopamine) Coatings

abbrev of surface types	DA (mg/mL)	P15 (mg/mL)	OGP (mg/mL)
P15/pDA/op-HA/PLGA	2	2	
op-HA/PLGA			
pDA/op-HA/PLGA	2		
OGP/pDA/op-HA/PLGA	2		0.1
P15/OGP/pDA/op-HA/PLGA	2	2	0.1
P15/OGP/op-HA/PLGA		2	0.1

2.6. Surface Characterization. FT-IR tests proceeded using a Bio-Rad Win-IR apparatus. X-ray photoelectron spectroscopy (XPS) (Thermo) was employed to detect the peptide-modified substrates. The elemental compositions of the modified substrates were obtained. An environmental scanning electron microscope (XL30, Philips) was utilized to access the surface topography of all the substrates. The water contact angle was measured on a Krüss DSA 10 instrument.

DOI: 10.1021/acsami.6b08733
ACS Appl. Mater. Interfaces 2016, 8, 26559−26569

Table 2. Primers Used in Quantitative Real-Time Polymerase Chain Reaction (qRT-PCR)

gene	forward primer sequence (5′−3′)	reverse primer sequence (5′−3′)
Runx2	GCCGGGAATGATGAGAACTA	GGACCGTCCACTGTCACTTT
OCN	AAGCAGGAGGGCAATAAGGT	TTTGTAGGCGGTCTTCAAGC
OPN	TCAGGACAACAACGGAAAGGG	GGAACTTGCTTGACTATCGATCAC
GAPDH	AACTTTGGCATTGTGGAAGG	ACACATTGGGGGTAGGAACA

Briefly, 10 μL of deionized water was dropped onto the sample surfaces. The shape of the water drop was recorded and measured.

2.7. Cell Culture. Cell experiments were performed by using mouse preosteoblasts (MC3T3-E1). Components of the medium and operation specifications for cell culture were in accordance with the previous study.[7]

2.8. Cell Morphology and Proliferation. After seeding 5×10^4 cells for each sample and incubation for 4, 24, and 48 h, cell fixation was conducted with 4% paraformaldehyde (PFA) in PBS for 15 min followed by rinsing three times. Afterward, it was hatched with fluorescein isothiocyanate (0.5 mg·mL^{-1} in DMSO) for 5 min and rinsed repeatedly. The morphological description of cell adhesion and migration on the substrate was captured as previously described[43]

By seeding 5×10^4 cells on each substrate and incubation for 1 and 7 days, the relative cell proliferation rate was studied via Cell Counting Kit-8 (CCK-8, Dojindo) according to the literature method (see the Supporting Information).[34]

2.9. Alkaline Phosphate (ALP) Activity Test. After incubating for 7 and 14 days on various substrates, cellular ALP activity was investigated via pNPP assay as described in the literature.[42,44] MC3T3-E1 cells were rinsed repeatedly with PBS and split by repeating freeze and thawing. A 500 μL portion of pNPP solution was placed in every well away from light and maintained at 37 °C for 0.5 h. The spectrophotometric values at 405 nm were determined via a full wavelength reader (Infinite M200, TECAN).

2.10. Calcium Deposition. von Kossa staining was performed to assess the calcium deposition by MC3T3-E1 cells incubated on the substrates for 14 days. After washing three times with phosphate buffer, the samples were fixed as described in section 2.8. The fixed cells were subjected to a 5% solution of $AgNO_3$ at 37 °C for 30 min followed by exposure to UV light with wavelength of 254 nm for 30 min. Then UV irradiated samples were rinsed repeatedly to remove unused $AgNO_3$ and kept in a 5% (w/v) solution of $Na_2S_2O_3$ for 10 min. In the end, the samples were gently rinsed repeatedly followed by redyeing with 1% (w/v) Neutral Red solution followed by rinsing with PBS twice. Digital images of stained cells were captured by a microscope (AX10, ZEISS) fitted with a camera (Imager A2, ZEISS). Nine photos for each sample were captured at random and the colored region was analyzed with NIH ImageJ.

2.11. Osteogenic Genes Expression. MC3T3-E1 cells were incubated on various substrates for 7 and 14 days. The expression of osteogenic genes was explored via quantitative real-time polymerase chain reaction (qRT-PCR). The extraction of RNA and analysis by qRT-PCR was conducted according to the literature methods.[7] The primers of osteogenic genes are shown in Table 2, comprising Runx2, OCN, and OPN. More details of the experiments were given in the Supporting Information.

2.12. Immunofluorescence Staining. MC3T3-E1 cells incubated on various substrates for 7 days were fixed as described in section 2.8. The samples were permeated with 0.1% Triton-X 100 in phosphate buffer for 5 min. After being blocked using 1% BSA in phosphate buffer for 30 min, the samples were incubated with primary antibody (OPN and Runx2, 1:500, Abcam) for 60 min under ambient temperature.[1] Subsequently, the samples were rinsed three times followed by incubation in fluorescein isothiocyanate (FITC)-labeled secondary antibody (1:500, Abcam) under ambient temperature for 60 min. Then the samples were stained with rhodamine−phalloidin (Cytoskeleton, Inc.) for 30 min under ambient temperature to visualize filamentous actin (F-actin), and cell nuclei were dyed with 4′,6-diamidino-2-phenylindole (DAPI). Photos were taken on a confocal laser scanning microscope (LSM 780, ZEISS).

2.13. Statistical Analysis. The data were analyzed using Origin 8.0 and are presented as the mean ± standard deviation. The statistic difference was evaluated by variance analysis (ANOVA one-way, Origin 8.0). A value of $p < 0.05$ was regarded as statistically significant.

3. RESULTS

3.1. Surface Characterization of P15- and OGP-Modified Composites via pDA coating. The chemical deposition of the modified op-HA/PLGA composite surfaces from FT-IR and XPS analyses demonstrated the efficient immobilization of peptides (Figure S1 of the Supporting Information and Table 3). FT-IR spectra of substrates coated with peptides are shown in Figure S1 (Supporting Information). The peak at 1596 cm^{-1}, which corresponds to the C═O stretching vibration (amide I) and N−H bending vibration (amide II), attributed to the amide bonds of peptides,[23] indicated successful incorporation of peptides on the substrates via pDA coating (Figure S1c−e, Supporting Information). Table 3 shows the elemental composition before and after peptide coating. The presence of nitrogen element (6.48%) indicated that pDA was successfully coated onto the op-HA/PLGA substrate. Incorporation of P15 and OGP peptides via pDA coating further increased the nitrogen content to 15.45% (P15/op-HA/PLGA), 10.53% (OGP/op-HA/PLGA), and 13.8% (P15/OGP/pDA/op-HA/PLGA), respectively, which benefited from the nitrogen-rich P15 and OGP peptides. It was interesting that the physically adsorbed P15 and OGP peptides were revealed by the appearance of the nitrogen element on the op-HA/PLGA substrate (12.37%), but the peak at 1596 cm^{-1} was not detected in FT-TR test. Probably, the physically adsorbed peptides were nonuniform, unstable, and easy to lose. This hypothesis was verified in the following cell experiments.

Table 3. Surface Chemical Composition (atomic concentration in %) of pDA-Coated op-HA/PLGA Substrates Analyzed by XPS

	C	O	N
op-HA/PLGA	62.63	31.55	
pDA/op-HA/PLGA	68.56	24.31	6.48
P15/pDA/op-HA/PLGA	62.17	21.56	15.45
OGP/pDA/op-HA/PLGA	65.12	22.9	10.53
P15/OGP/pDA/op-HA/PLGA	65.48	19.64	13.8
P15/OGP/op-HA/PLGA	62.72	23.49	12.37

ESEM images showed that surface microtopography and roughness of the substrates were obviously improved by pDA coating (Figure S2, Supporting Information). As shown in Figure S2a, most of the op-HA filler was embedded within the matrix. The surface topography of the substrates was influenced by pDA coating, and a large amount of polymerized DA particles was found on the pDA-coated or pDA-mediated peptide-immobilized substrates (Figure S2b−e). So the surface roughness of the substrates was increased. The same results were also reported in the literature and the pDA coating might alter the surface performances of the polymer matrix, including

DOI: 10.1021/acsami.6b08733
ACS Appl. Mater. Interfaces 2016, 8, 26559−26569

surface roughness and hydrophilicity.[33] The surface microtopography of sample f was not changed obviously compared with that of bare op-HA/PLGA (Figure S2f). The water contact angles for the op-HA/PLGA samples with pDA modification were obviously decreased compared with those of the bare op-HA/PLGA samples, with a statistically significant difference ($p < 0.05$, Figure 1). The average water contact angle dramatically

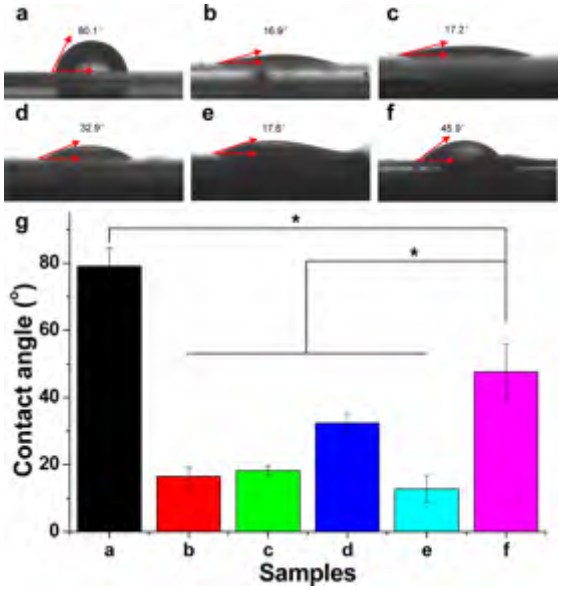

Figure 1. Water contact angle measurement for the composites (a) op-HA/PLGA, (b) pDA/op-HA/PLGA, (c) P15/pDA/op-HA/PLGA, (d) OGP/pDA/op-HA/PLGA, (e) P15/OGP/pDA/op-HA/PLGA, and (f) P15/OGP/op-HA/PLGA. (g) Average water contact angle analysis. Asterisks (*) indicate statistical significance, $p < 0.05$.

decreased from 79.10° ± 5.37° for the op-HA/PLGA samples to 16.45° ± 2.72° for the pDA/op-HA/PLGA samples with the pDA coating, indicating a significant increase of wettability due to the pDA coating on the substrates ($p < 0.05$, Figure 1a,b,g). The contact angle was further decreased after pDA-mediated peptides' immobilization ($p < 0.05$, Figure 1b–e). The water contact angle of the substrates with physically adsorbed peptides was dramatically lower than that of bare op-HA/PLGA samples ($p < 0.05$, Figure 1a,f). This indicated that the wettability of op-HA/PLGA substrates was improved by the adsorbed peptides to some extent. However, the increase of wettability of op-HA/PLGA substrates by pDA coating with or without P15 and OGP peptides was more obvious than that of bare op-HA/PLGA samples or physically adsorbed peptides. The P15/OGP/pDA/op-HA/PLGA sample showed the maximum wettability, attributed to the combined effect of the surface roughness that was improved by pDA coating and pDA-mediated peptide immobilization. However, a statistical difference was not observed for the wettability among all the pDA-coated groups ($p > 0.05$, Figure 1b–e).

3.2. Cell Morphology and Proliferation on P15-Modified Composites via pDA coating. Enhancement of cell adhesion and proliferation on the grafts is a crucial factor for promoting osseointegration.[14] Cell-adhesive peptides, such as collagen mimetic peptide (P15), have an ability to bind cell membrane integrins followed by mediating cell adhesion.[18] So, we first investigated the cell adhesion, morphology, and proliferation with P15 immobilization via pDA coating compared with the bare op-HA/PLGA or only-pDA-coated substrates. MC3T3-E1 cells were fluorescently stained to investigate cell adhesion and migration behavior on the P15 incorporated materials. The attachment of cells cultured on pDA/op-HA/PLGA and P15/pDA/op-HA/PLGA substrates was better compared with that on op-HA/PLGA and P15/op-HA/PLGA substrates due to the hydrophilic enhancement upon pDA coating and immobilization of P15 peptide, respectively (Figure 2A,B). Additionally, the cell adhesion on the P15/pDA/op-HA/PLGA composites was also better than that of the pDA/op-HA/PLGA composites at any time point (Figure 2A,B), which likely contributed to the formation of focal adhesions benefiting from P15 peptide. However, the cell adhesion was unsatisfactory with physically adsorbed P15 peptide on the op-HA/PLGA composite substrates.

The relative cell proliferation rate, compared to that of the bare op-HA/PLGA group, was observed to raise with the increase of incubation time on pDA/op-HA/PLGA and P15/pDA/op-HA/PLGA composites (Figure 2C). The cell proliferation was significantly greater in the pDA/op-HA/PLGA and P15/pDA/op-HA/PLGA groups compared to P15/op-HA/PLGA at 1 and 7 days ($p < 0.05$, Figure 2C). Furthermore, a statistical difference in cell proliferation was observed between the pDA/op-HA/PLGA and P15/pDA/op-HA/PLGA groups ($p < 0.05$, Figure 2C). The cell proliferation was much lower on the substrates of physically adsorbed P15 peptide at 7 days. Thus, these results indicated that P15 immobilization accomplished by the biomimetic coating process promoted MC3T3-E1 cell proliferation on the op-HA/PLGA composites.

3.3. Alkaline Phosphatase (ALP) Activity. The high reactivity of ALP represented osteodifferentiation of cells.[45] Hence, it could be regarded as the osteoinductive activity of the peptides' functional substrates. It was noted that OGP could dramatically up-regulate the reactivity of ALP in hMSCs.[8] Figure 3 showed the reactivity of ALP in MC3T3-E1 cells on the various materials. An obvious rise in ALP reactivity of MC3T3-E1 cells was noticed on the OGP- or P15/OGP-modified substrates, being superior to the samples of bare op-HA/PLGA and pDA-coated and P15-immobilized substrates at both 7 and 14 days. It demonstrated that the osteodifferentiation ability was stronger for the OGP-modified substrates than others. In addition, the ALP reactivity of MC3T3-E1 cells on P15-modified substrates was significantly better than that of bare op-HA/PLGA at 14 days ($p < 0.05$, Figure 3).

3.4. Calcium Deposition. Levels of calcium deposition were evaluated by von Kossa staining, as shown in Figure 4. There was little mineral deposition on bare op-HA/PLGA and substrates with physically adsorbed peptides after 14 days of culturing (Figure 4a,f), whereas calcium deposition was greater on pDA-coated substrates (Figure 4b–e). Especially the substrates incorporating P15, OGP, and P15/OGP peptides exhibited the largest and most organized nodules, indicating that the differentiation of MC3T3-E1 cells was enhanced. Consistently matching the images, morphological analysis indicated that incorporation of peptides via pDA coating significantly expanded the mineralized area (op-HA/PLGA, 11.16 ± 8.13%; P15/pDA/op-HA/PLGA, 48.14 ± 16.15%; OGP/pDA/op-HA/PLGA, 53.53 ± 11.29%; P15/OGP/pDA/op-HA/PLGA, 55.61 ± 16.18%) (Figure 4g).

3.5. Bone-Related Gene Expression by qRT-PCR Tests. Cell osteodifferentiation was evaluated at 7 and 14 days with osteogenic gene expression. The expression of Runx2 in the

DOI: 10.1021/acsami.6b08733
ACS Appl. Mater. Interfaces 2016, 8, 26559–26569

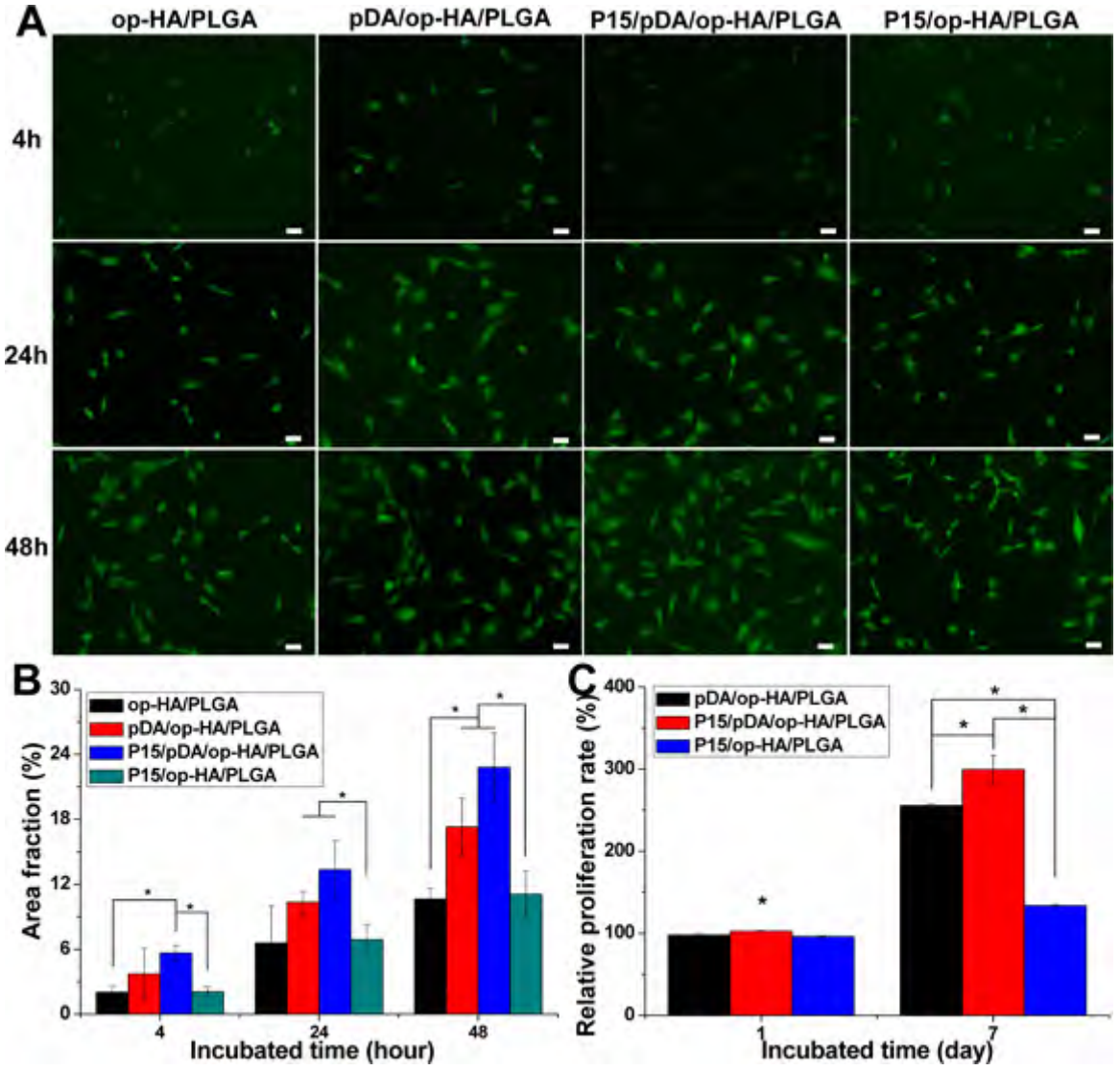

Figure 2. Morphology (A) and area fraction (B) of MC3T3-E1 cells cultured on op-HA/PLGA, pDA/op-HA/PLGA, P15/pDA/op-HA/PLGA, and P15/op-HA/PLGA substrates for 4, 24, and 48 h. Scale bar lengths are 100 μm. The relative proliferation rate (C) of MC3T3-E1 cells cultured on pDA/op-HA/PLGA, P15/pDA/op-HA/PLGA, and P15/op-HA/PLGA compared to op-HA/PLGA substrates for 1 and 7 days. Asterisks (*) indicate statistical significance, $p < 0.05$.

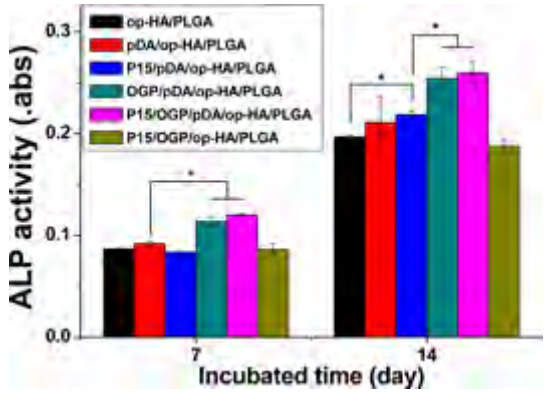

Figure 3. Alkaline phosphatase activity of MC3T3-E1 cells on the different substrates at 7 and 14 days. Asterisks (*) indicate statistical significance, $p < 0.05$.

P15/OGP-modified samples was obviously higher than that of the other groups at 7 days ($p < 0.05$, Figure 5A). The levels of OPN gene expression from the OGP- and P15/OGP-modified groups were dramatically stronger than those of the other groups at 7 days ($p < 0.05$, Figure 5A). A little higher OCN gene expression at 7 days on pDA/op-HA/PLGA, OGP/pDA/op-HA/PLGA, and P15/OGP/pDA/op-HA/PLGA groups was observed without significant difference ($p > 0.05$, Figure 5A). Furthermore, the expression of Runx2 and OCN was stronger for the P15/OGP/pDA/op-HA/PLGA samples at 14 days ($p > 0.05$, Figure 5B). The OPN gene expression was higher in P15-, OGP-, and P15/OGP-modified groups via pDA coating ($p > 0.05$, Figure 5B). Findings in this study showed that the modification with P15 and OGP peptides via pDA coating on the substrates enhanced osteodifferentiation of MC3T3-E1 cells.

3.6. Bone-Related Protein Expression by Immunofluorescence Staining. The protein expression of osteogenic factors (OPN and Runx2) on the different substrates is shown in Figure 6. Even though the wettability of op-HA/PLGA substrate was improved via pDA coating, as mentioned above, both OPN and Runx2 expression were slightly higher for bare

DOI: 10.1021/acsami.6b08733
ACS Appl. Mater. Interfaces 2016, 8, 26559−26569

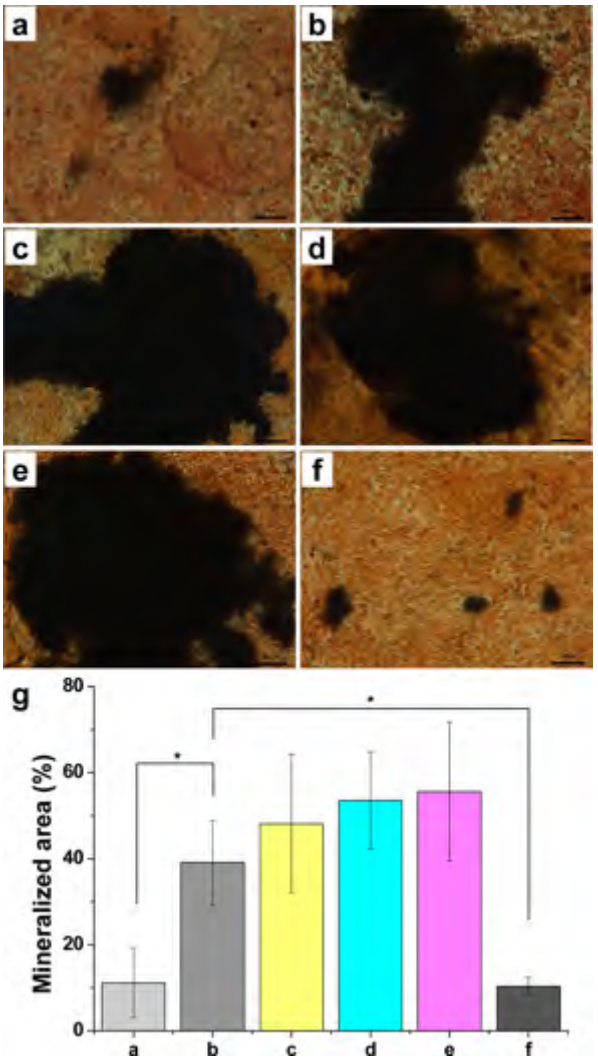

Figure 4. Calcium deposition evaluated by von Kossa staining of MC3T3-E1 cells cultured on the different substrates of (a) op-HA/PLGA, (b) pDA/op-HA/PLGA, (c) P15/pDA/op-HA/PLGA, (d) OGP/pDA/op-HA/PLGA, (e) P15/OGP/pDA/op-HA/PLGA, and (f) P15/OGP/op-HA/PLGA for 14 days. Scale bar lengths are 100 μm. (g) Morphometric analysis of von Kossa staining. Asterisks (*) indicate statistical significance, $p < 0.05$.

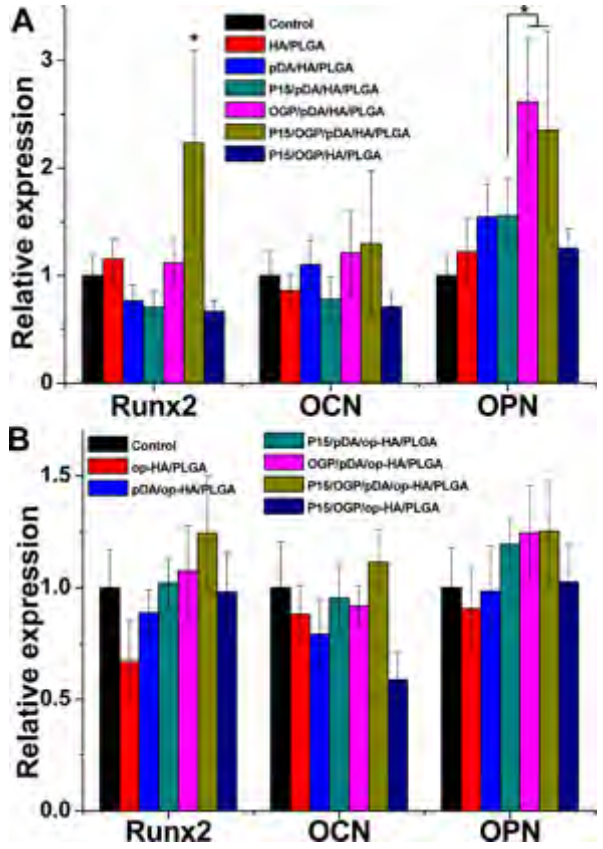

Figure 5. MC3T3-E1 cells were cultured on the different substrates for 7 (A) and 14 (B) days. The expression of three osteogenic genes (Runx2, OCN, and OPN) was analyzed by qRT-PCR. The intensity of each gene was normalized to the value of GADPH. Asterisks (*) indicate statistical significance, $p < 0.05$.

op-HA/PLGA than for the pDA/op-HA/PLGA samples at 7 days (Figure 6). Upon the incorporation of OGP or P15/OGP on the substrates, more OPN and Runx2 expression was observed according to the fluorescence images. The OPN and Runx2 expression levels from the P15/OGP/pDA/op-HA/PLGA group were even higher than that of the OGP/pDA/op-HA/PLGA group. The protein expression is highly consistent with the observation of ALP activity, calcium deposits, and bone-related gene expression.

4. DISCUSSION

A major aim of the work was to improve cell adhesion and osteogenic activity on bone implants for osteointegration. Upon modification, we demonstrated that incorporation of P15 and OGP peptides via a pDA-coating method enhanced cell attachment, spreading, proliferation, and osteodifferentiation. First, we made a comparison about the effectiveness of peptide immobilization with the help of pDA coating and physical adsorption. XPS analysis showed that the nitrogen content of substrates with peptides immobilized via pDA coating was higher than that of bare op-HA/PLGA substrate and physically adsorbed peptides (Table 3). This indicated that pDA-assisted immobilization resulted in large amount of peptides coated on the materials, as inspired by the distinctive adhesion mechanism in mussels. Chien and Tsai reported that bone morphogenic protein-2 (BMP-2) was incorporated by a poly(dopamine)-coating process and the nitrogen element was increased, as demonstrated by XPS.[14] In another study, polymerized DA particles were noted on the PLGA film coated with pDA, and the surface roughness and wettability were changed.[33] A similar phenomenon was also observed in this study, and the pDA particles appeared on the pDA-coated substrate, as shown in Figure S2 of the Supporting Information. Correspondingly, the wettability of pDA-coated op-HA/PLGA substrates was extraordinarily improved (Figure 1), especially for the P15/OGP/pDA/op-HA/PLGA substrate. Surface wettability was extremely important for cellular interaction with materials.[34,46,47] Therefore, the cell adhesion, spreading, and proliferation were increased to a certain degree by pDA coating on the substrate compared to the bare substrate.

Recently, immobilization of bioactive agents via pDA deposition was utilized for enhancement of cell adhesion, osteointegration, and osteogenesis of tissue-engineering substrates.[14,32−34,48] In the study, the cell adhesion, morphology, and proliferation with P15 peptide immobilization via pDA coating were investigated compared with those of the bare op-HA/PLGA or only-pDA-coated substrate. Most obviously, cell

DOI: 10.1021/acsami.6b08733
ACS Appl. Mater. Interfaces 2016, 8, 26559−26569

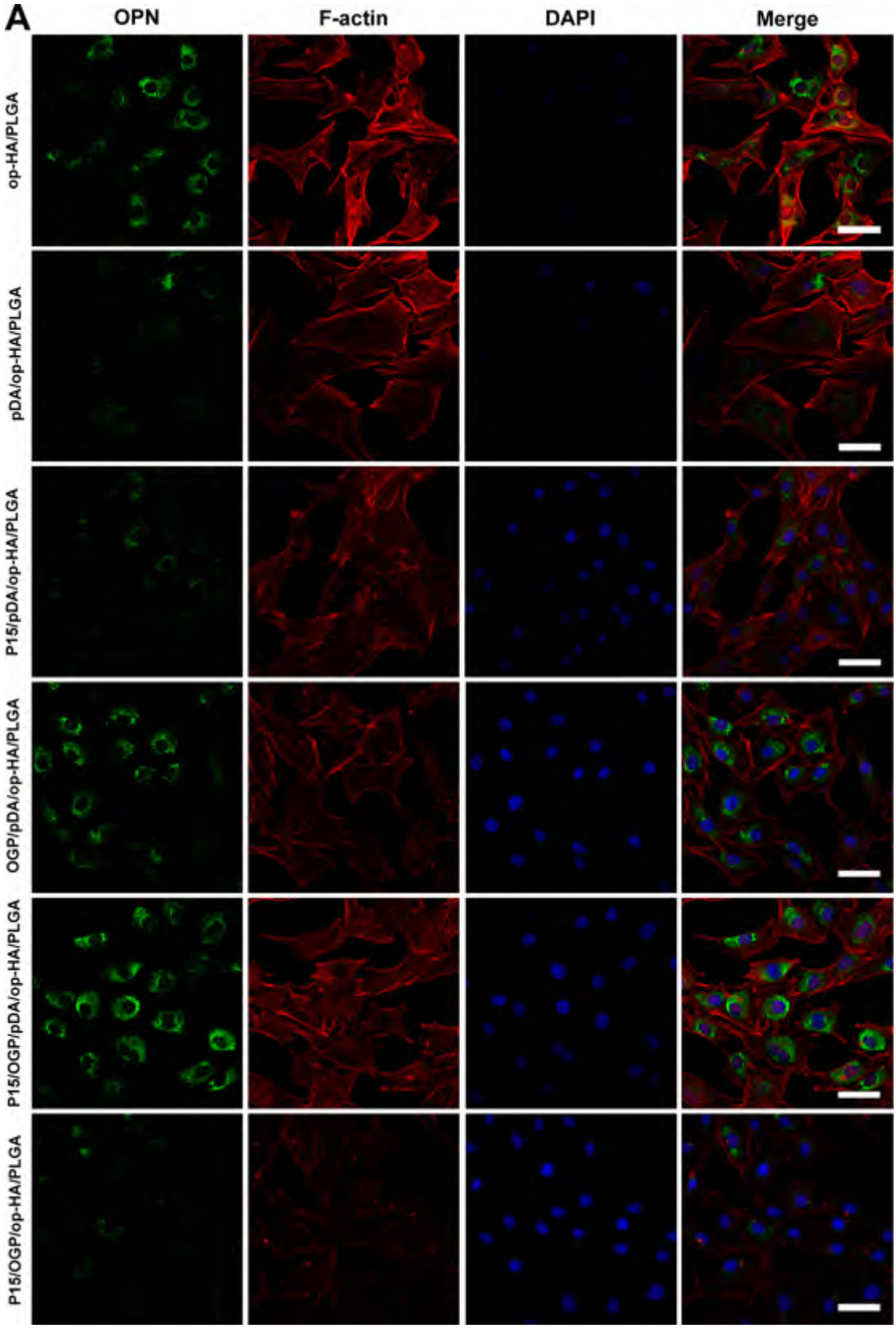

Figure 6. continued

DOI: 10.1021/acsami.6b08733
ACS Appl. Mater. Interfaces 2016, 8, 26559−26569

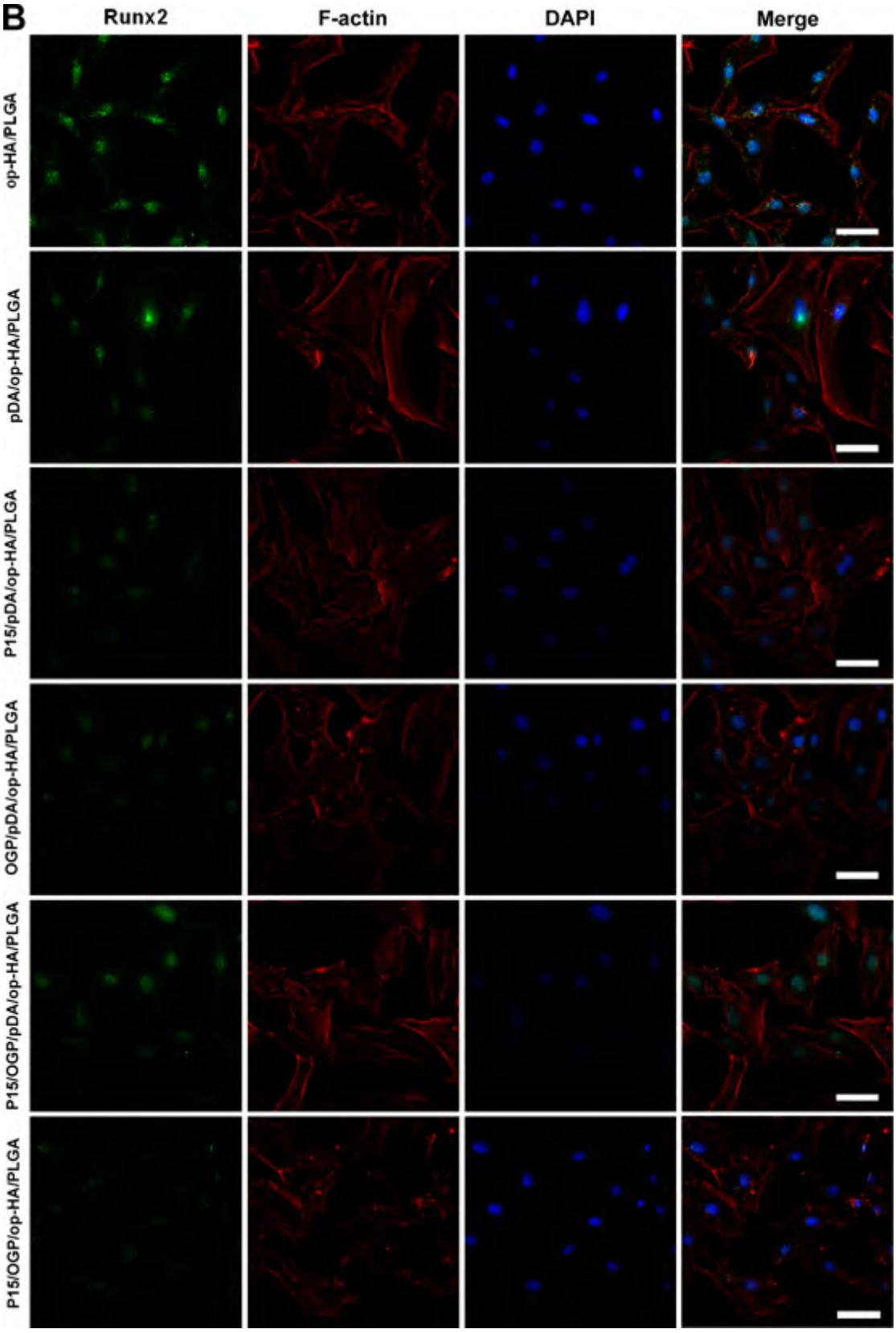

Figure 6. Immunofluorescent images of OPN (A) and Runx2 (B) expressed by MC3T3-E1 cells cultured on the different substrates for 7 days which were observed by a confocal laser scanning microscope. FITC-conjugated secondary antibody for OPN or Runx2 (green), phalloidin tetramethylrhodamine B isothiocyanate for actin microfilaments (red), and DAPI staining for nuclei (blue). Scale bar lengths are 50 μm.

adhesion, spreading, and proliferation were significantly promoted by P15 peptide immobilization (Figure 2). This is because collagen mimetic peptides, including P15, have an ability to bind cell membrane integrins followed by mediating

DOI: 10.1021/acsami.6b08733
ACS Appl. Mater. Interfaces 2016, 8, 26559−26569

cell adhesion. Hennessy et al. found that compared to bare HA substrates, MSCs experienced dramatically superior adhesion compared to that with P15 coating. This was in accord with the recognized character of P15 by means of integrin-binding factor.[18] Liu et al. reported that the P15-peptide-modified titanium surface appeared to functionalize in the form of improving cell adhesion and osteodifferentiation.[20] Also, P15-peptide-coated matrix in hydrogels also could enhance cell attachment and osteoblastic differentiation.[49] Thus, the improvement of wettability and immobilization of P15 peptide in this study enhanced cell adhesion, migration, and proliferation. Accordingly, cell adhesion and proliferation on the P15/OGP/pDA/op-HA/PLGA substrate would also be satisfactory owing to efficient immobilization of peptides via pDA coating.

Apart from cell adhesion and proliferation, osteodifferentiation was also crucial for bone regeneration. According to the literature, P15 peptide quickened early bone regeneration of anorganic bone matrix for repair of a large bone defect in pigs.[18] OGP peptide enhanced the osteoinductive potential of mesenchymal stem cells and accelerated bony regeneration[8,9,31] In this study, OGP was codeposited onto the substrate via the pDA-coating method. It was expected that OGP peptide would increase osteogenic activity together with P15 peptide and op-HA nanoparticles in the composite for bone regeneration. Incorporation of P15 and OGP peptides on the substrates was first evaluated using the ALP reactivity test. After incubating for 7 and 14 days, ALP reactivity was significantly up-regulated for the OGP/pDA/op-HA/PLGA and P15/OGP/pDA/op-HA/PLGA substrates (Figure 3), indicating the osteoinductivity of surface-immobilized OGP and P15/OGP peptides via poly(dopamine) deposition. In the previous studies, ALP reactivity was also enhanced by incorporation of OGP, indicating that incorporated OGP stimulated osteogenic differentiation, especially in the early stage.[8,9,27] von Kossa staining also showed mineralization for the P15-, OGP-, or P15/OGP-immobilized substrates via pDA coating for 14 days (Figure 4). Positive von Kossa staining has been used to indicate osteodifferentiation.[50,51] Calcium deposition of osteodifferentiated cells was also noticed by pDA-assisted BMP-2 peptide incorporation on PLGA materials, indicating promotion of osteodifferentiation of hADSCs.[33]

The peptide-modified substrates were further tested using qRT-PCR analysis and immunofluorescence staining of several osteogenic markers to assess the osteodifferentiation of MC3T3-E1 cells. Quantitative analysis of Runx2, OCN, and OPN supported the results from ALP reactivity and mineralization. Runx2 and OPN are both critical tags for osteodifferentiation of BMSCs.[52] OCN is known as the most specific protein for osteogenic matrix maturation and is viewed as a marker for bone formation.[53] When P15 and OGP peptides were introduced via pDA coating, the expression of osteogenic genes was obviously stronger than that of the other groups, implying that the immobilization of peptides via pDA coating was favorable for early stage osteodifferentiation of MC3T3-E1 cells in vitro. Higher and constant expression of Runx2 was also noted for OGP-functional poly(ester urea)s (PEU), suggesting a faster progression of osteogenesis.[9] In Chien and Tsai's study, the expression of Runx2 and OPN was both up-regulated by BMP-2 immobilization via pDA coating on Ti surface, indicating that the incorporation of BMP-2 enhanced the osteodifferentiation of cells.[14] Immunofluorescence staining of osteogenesis, chondrogenesis, or angiogenesis markers has been utilized for evaluation of relevant protein expression.[54−56] In this study, very little green fluorescence was observed on pDA/op-HA/PLGA surfaces, indicating that the OPN and Runx2 protein expression levels were a little lower than that on op-HA/PLGA substrate, perhaps because calcium and phosphorus exposure was affected by pDA coating to a certain extent. Upon the addition of OGP peptide, more OPN and Runx2 proteins were expressed on OGP/pDA/op-HA/PLGA and P15/OGP/pDA/op-HA/PLGA substrates (Figure 6). The above findings are consistent with the results of osteogenic gene expression. The cell differentiation study showed that the property of peptide-modified substrates played an important role in cellular activities of proliferation and osteodifferentiation. This was consistent with previous studies[8,9,27] in which OGP peptides have been demonstrated to promote the proliferation of osteoblast and MSC and quicken ossification.

Thus, we herein demonstrate that pDA-assisted immobilization of peptides is a promising method to modify the surface of op-HA/PLGA substrates for bone regeneration. The biomimetic coating process utilized in this study is simple but quite practical. In future work, this method should be improved for a more functional porous scaffold, and the biological properties of the peptide-modified op-HA/PLGA scaffolds need to be further investigated.

5. CONCLUSIONS

In this study, op-HA/PLGA composite substrate was successfully modified through pDA-assisted immobilization of P15 and OGP peptides using a mussel-inspired biomimetic coating process. The pDA-mediated functionalization allowed for dependable and efficient immobilization of peptides onto the substrates. In vitro studies including fluorescence staining, CCK-8 assay, ALP activity, calcium deposition, qRT-PCR analysis, and immunofluorescence staining indicated that the peptides coating the op-HA/PLGA substrates promoted adhesion, proliferation, and osteodifferentiation of MC3T3-E1 cells compared with the bare substrates. Therefore, the surfaces biofunctionalized with bioactive peptides can provide an attractive technology for modification of bone substitutes in orthopedic and dental applications.

■ ASSOCIATED CONTENT

Supporting Information

The Supporting Information is available free of charge on the ACS Publications website at DOI: 10.1021/acsami.6b08733.

Synthesis of polymer, surface grafting of n-HA, cell proliferation, osteogenic genes expression, FT-IR spectra, and ESEM images (PDF)

■ AUTHOR INFORMATION

Corresponding Author

*Phone/fax: +86 431 85262058. E-mail: zhangpb@ciac.ac.cn.

Notes

The authors declare no competing financial interest.

■ ACKNOWLEDGMENTS

This research was financially supported by National Natural Science Foundation of China (Projects 51403197, 51473164, and 51273195), the Ministry of Science and Technology of China (International Cooperation and Communication Program 2014DFG52510), the joint funded program of Chinese

DOI: 10.1021/acsami.6b08733
ACS Appl. Mater. Interfaces 2016, 8, 26559−26569

Academy of Sciences and Japan Society for the Promotion of Science (GJHZ1519) and the Program of Scientific Development of Jilin Province (20130201005GX).

REFERENCES

(1) Li, H.; Chen, S. Y.; Chen, J. W.; Chang, J.; Xu, M. C.; Sun, Y. Y.; Wu, C. T. Mussel-Inspired Artificial Grafts for Functional Ligament Reconstruction. *ACS Appl. Mater. Interfaces* **2015**, *7* (27), 14708−14719.
(2) Ducheyne, P.; Mauck, R. L.; Smith, D. H. Biomaterials in the Repair of Sports Injuries. *Nat. Mater.* **2012**, *11* (8), 652−654.
(3) Qiu, X. Y.; Hong, Z. K.; Hu, J. L.; Chen, L.; Chen, X. S.; Jing, X. B. Hydroxyapatite Surface Modified by L-lactic Acid and its Subsequent Grafting Polymerization of L-lactide. *Biomacromolecules* **2005**, *6* (3), 1193−1199.
(4) Dorozhkin, S. V. Bioceramics of Calcium Orthophosphates. *Biomaterials* **2010**, *31* (7), 1465−1485.
(5) Kim, S. S.; Park, M. S.; Gwak, S. J.; Choi, C. Y.; Kim, B. S. Accelerated Bonelike Apatite Growth on Porous Polymer/Ceramic Composite Scaffolds in Vitro. *Tissue Eng.* **2006**, *12* (10), 2997−3006.
(6) Choi, S. Y.; Murphy, W. L. The Effect of Mineral Coating Morphology on Mesenchymal Stem Cell Attachment and Expansion. *J. Mater. Chem.* **2012**, *22* (48), 25288−25295.
(7) Wang, Z. L.; Xu, Y.; Wang, Y.; Ito, Y.; Zhang, P. B.; Chen, X. S. Enhanced in Vitro Mineralization and in Vivo Osteogenesis of Composite Scaffolds through Controlled Surface Grafting of L-Lactic Acid Oligomer on Nanohydroxyapatite. *Biomacromolecules* **2016**, *17* (3), 818−829.
(8) Maia, F. R.; Barbosa, M.; Gomes, D. B.; Vale, N.; Gomes, P.; Granja, P. L.; Barrias, C. C. Hydrogel Depots for Local Co-delivery of Osteoinductive Peptides and Mesenchymal Stem Cells. *J. Controlled Release* **2014**, *189*, 158−168.
(9) Policastro, G. M.; Lin, F.; Smith Callahan, L. A.; Esterle, A.; Graham, M.; Stakleff, K. S.; Becker, M. L. OGP Functionalized Phenylalanine-Based Poly(ester urea) for Enhancing Osteoinductive Potential of Human Mesenchymal Stem Cells. *Biomacromolecules* **2015**, *16* (4), 1358−1371.
(10) Scarfì, S. Use of Bone Morphogenetic Proteins in Mesenchymal Stem Cell Stimulation of Cartilage and Bone Repair. *World journal of stem cells* **2016**, *8* (1), 1−12.
(11) Farokhi, M.; Mottaghitalab, F.; Shokrgozar, M. A.; Ou, K. L.; Mao, C. B.; Hosseinkhani, H. Importance of Dual Delivery Systems for Bone Tissue Engineering. *J. Controlled Release* **2016**, *225*, 152−169.
(12) Shimer, A. L.; Oner, F. C.; Vaccaro, A. R. Spinal Reconstruction and Bone Morphogenetic Proteins: Open Questions. *Injury* **2009**, *40*, S32−S38.
(13) Firestone, A. J.; Chen, J. K. Controlling Destiny through Chemistry: Small-Molecule Regulators of Cell Fate. *ACS Chem. Biol.* **2010**, *5* (1), 15−34.
(14) Chien, C. Y.; Tsai, W. B. Poly(dopamine)-Assisted Immobilization of Arg-Gly-Asp Peptides, Hydroxyapatite, and Bone Morphogenic Protein-2 on Titanium to Improve the Osteogenesis of Bone Marrow Stem Cells. *ACS Appl. Mater. Interfaces* **2013**, *5* (15), 6975−6983.
(15) Zhang, P. B.; Wu, H. T.; Wu, H.; Lu, Z. W.; Deng, C.; Hong, Z. K.; Jing, X. B.; Chen, X. S. RGD-Conjugated Copolymer Incorporated into Composite of Poly(lactide-co-glycotide) and Poly(L-lactide)-Grafted Nanohydroxyapatite for Bone Tissue Engineering. *Biomacromolecules* **2011**, *12* (7), 2667−2680.
(16) Sawyer, A. A.; Hennessy, K. M.; Bellis, S. L. Regulation of Mesenchymal Stem Cell Attachment and Spreading on Hydroxyapatite by RGD Peptides and Adsorbed Serum Proteins. *Biomaterials* **2005**, *26* (13), 1467−1475.
(17) Hennessy, K. M.; Clem, W. C.; Phipps, M. C.; Sawyer, A. A.; Shaikh, F. M.; Bellis, S. L. The Effect of RGD Peptides on Osseointegration of Hydroxyapatite Biomaterials. *Biomaterials* **2008**, *29* (21), 3075−3083.
(18) Hennessy, K. M.; Pollot, B. E.; Clem, W. C.; Phipps, M. C.; Sawyer, A. A.; Culpepper, B. K.; Bellis, S. L. The Effect of Collagen I Mimetic Peptides on Mesenchymal Stem Cell Adhesion and Differentiation, and on Bone Formation at Hydroxyapatite Surfaces. *Biomaterials* **2009**, *30* (10), 1898−1909.
(19) Long, M.; Rack, H. J. Titanium Alloys in Total Joint Replacement - A Materials Science Perspective. *Biomaterials* **1998**, *19* (18), 1621−1639.
(20) Liu, Q. Y.; Limthongkul, W.; Sidhu, G.; Zhang, J.; Vaccaro, A.; Shenck, R.; Hickok, N.; Shapiro, I.; Freeman, T. Covalent Attachment of P15 Peptide to Titanium Surfaces Enhances Cell Attachment, Spreading, and Osteogenic Gene Expression. *J. Orthop. Res.* **2012**, *30* (10), 1626−1633.
(21) Hanks, T.; Atkinson, B. L. Comparison of Cell Viability on Anorganic Bone Matrix with or without P-15 Cell Binding Peptide. *Biomaterials* **2004**, *25* (19), 4831−4836.
(22) Bhatnagar, R. S.; Qian, J. J.; Gough, C. A. The Role in Cell Binding of A Beta-bend within the Triple Helical Region in Collagen Alpha 1(I) Chain: Structural and Biological Evidence for Conformational Tautomerism on Fiber Surface. *J. Biomol. Struct. Dyn.* **1997**, *14* (5), 547−560.
(23) Zhou, X.; Feng, W.; Qiu, K.; Chen, L.; Wang, W.; Nie, W.; Mo, X.; He, C. BMP-2 Derived Peptide and Dexamethasone Incorporated Mesoporous Silica Nanoparticles for Enhanced Osteogenic Differentiation of Bone Mesenchymal Stem Cells. *ACS Appl. Mater. Interfaces* **2015**, *7* (29), 15777−89.
(24) Bab, I.; Gavish, H.; Namdar-Attar, M.; Muhlrad, A.; Greenberg, Z.; Chen, Y.; Mansur, N.; Shteyer, A.; Chorev, M. Isolation of Mitogenically Active C-terminal Truncated Pentapeptide of Osteogenic Growth Peptide from Human Plasma and Culture Medium of Murine Osteoblastic Cells. *J. Pept. Res.* **1999**, *54* (5), 408−14.
(25) Chen, Z. X.; Wang, X. F.; Shao, Y. C.; Shi, D. Y.; Chen, T. Y.; Cui, D. F.; Jiang, X. X. Synthetic Osteogenic Growth Peptide Promotes Differentiation of Human Bone Marrow Mesenchymal Stem Cells to Osteoblasts via RhoA/ROCK Pathway. *Mol. Cell. Biochem.* **2011**, *358* (1−2), 221−227.
(26) Bab, I.; Smith, E.; Gavish, H.; Attar-Namdar, M.; Chorev, M.; Chen, Y. C.; Muhlrad, A.; Birnbaum, M. J.; Stein, G.; Frenkel, B. Biosynthesis of Osteogenic Growth Peptide via Alternative Translational Initiation at AUG(85) of Histone H4 mRNA. *J. Biol. Chem.* **1999**, *274* (20), 14474−14481.
(27) Chen, C.; Kong, X. D.; Zhang, S. M.; Lee, I. S. Characterization and in Vitro Biological Evaluation of Mineral/Osteogenic Growth Peptide Nanocomposites Synthesized Biomimetically on Titanium. *Appl. Surf. Sci.* **2015**, *334*, 62−68.
(28) Mendes, L. S.; Saska, S.; Martines, M. A. U.; Marchetto, R. Nanostructured Materials Based on Mesoporous Silica and Mesoporous Silica/Apatite as Osteogenic Growth Peptide Carriers. *Mater. Sci. Eng., C* **2013**, *33* (7), 4427−4434.
(29) Gabet, Y.; Muller, R.; Regev, E.; Sela, J.; Shteyer, A.; Salisbury, K.; Chorev, M.; Bab, I. Osteogenic Growth Peptide Modulates Fracture Callus Structural and Mechanical Properties. *Bone* **2004**, *35* (1), 65−73.
(30) Brager, M. A.; Patterson, M. J.; Connolly, J. F.; Nevo, Z. Osteogenic Growth Peptide Normally Stimulated by Blood Loss and Marrow Ablation Has Local and Systemic Effects on Fracture Healing in Rats. *J. Orthop. Res.* **2000**, *18* (1), 133−139.
(31) Zhao, Z. Y.; Shao, L.; Zhao, H. M.; Zhong, Z. H.; Liu, J. Y.; Hao, C. G. Osteogenic Growth Peptide Accelerates Bone Healing During Distraction Osteogenesis in Rabbit Tibia. *J. Int. Med. Res.* **2011**, *39* (2), 456−463.
(32) Tsai, W. B.; Chen, W. T.; Chien, H. W.; Kuo, W. H.; Wang, M. J. Poly(dopamine) Coating of Scaffolds for Articular Cartilage Tissue Engineering. *Acta Biomater.* **2011**, *7* (12), 4187−4194.
(33) Ko, E.; Yang, K.; Shin, J.; Cho, S. W. Polydopamine-Assisted Osteoinductive Peptide Immobilization of Polymer Scaffolds for Enhanced Bone Regeneration by Human Adipose-Derived Stem Cells. *Biomacromolecules* **2013**, *14* (9), 3202−3213.
(34) Li, Y.; Yang, W.; Li, X. K.; Zhang, X.; Wang, C. R.; Meng, X. F.; Pei, Y. F.; Fan, X. L.; Lan, P. H.; Wang, C. H.; Li, X. J.; Guo, Z. Improving Osteointegration and Osteogenesis of Three-Dimensional

DOI: 10.1021/acsami.6b08733
ACS Appl. Mater. Interfaces 2016, 8, 26559−26569

Porous Ti6AI4V Scaffolds by Polydopamine-Assisted Biomimetic Hydroxyapatite Coating. *ACS Appl. Mater. Interfaces* **2015**, *7* (10), 5715−5724.
(35) Liu, Y. L.; Ai, K. L.; Lu, L. H. Polydopamine and Its Derivative Materials: Synthesis and Promising Applications in Energy, Environmental, and Biomedical Fields. *Chem. Rev.* **2014**, *114* (9), 5057−5115.
(36) Madhurakkat Perikamana, S. K. M.; Lee, J.; Lee, Y. B.; Shin, Y. M.; Lee, E. J.; Mikos, A. G.; Shin, H. Materials from Mussel-Inspired Chemistry for Cell and Tissue Engineering Applications. *Biomacromolecules* **2015**, *16* (9), 2541−2555.
(37) Gao, X.; Song, J. L.; Ji, P.; Zhang, X. H.; Li, X. M.; Xu, X.; Wang, M. K.; Zhang, S. Q.; Deng, Y.; Deng, F.; Wei, S. C. Polydopamine-Templated Hydroxyapatite Reinforced Polycaprolactone Composite Nanofibers with Enhanced Cytocompatibility and Osteogenesis for Bone Tissue Engineering. *ACS Appl. Mater. Interfaces* **2016**, *8* (5), 3499−3515.
(38) Lee, H.; Lee, B. P.; Messersmith, P. B. A Reversible Wet/Dry Adhesive Inspired by Mussels and Geckos. *Nature* **2007**, *448* (7151), 338−U4.
(39) Sedo, J.; Saiz-Poseu, J.; Busque, F.; Ruiz-Molina, D. Catechol-Based Biomimetic Functional Materials. *Adv. Mater.* **2013**, *25* (5), 653−701.
(40) Hong, Z. K.; Zhang, P. B.; Liu, A. X.; Chen, L.; Chen, X. S.; Jing, X. B. Composites of Poly(lactide-co-glycolide) and the Surface Modified Carbonated Hydroxyapatite Nanoparticles. *J. Biomed. Mater. Res., Part A* **2007**, *81A* (3), 515−522.
(41) Qiu, X. Y.; Chen, L.; Hu, J. L.; Sun, J. R.; Hong, Z. K.; Liu, A. X.; Chen, X. S.; Jing, X. B. Surface-modified Hydroxyapatite Linked by L-lactic Acid Oligomer in the Absence of Catalyst. *J. Polym. Sci., Part A: Polym. Chem.* **2005**, *43* (21), 5177−5185.
(42) Gao, T. L.; Zhang, N.; Wang, Z. L.; Wang, Y.; Liu, Y.; Ito, Y.; Zhang, P. B. Biodegradable Microcarriers of Poly(Lactide-co-Glycolide) and Nano-Hydroxyapatite Decorated with IGF-1 via Polydopamine Coating for Enhancing Cell Proliferation and Osteogenic Differentiation. *Macromol. Biosci.* **2015**, *15* (8), 1070−1080.
(43) Cui, Y.; Liu, Y.; Cui, Y.; Jing, X. B.; Zhang, P. B. A.; Chen, X. S. The Nanocomposite Scaffold of Poly(lactide-co-glycolide) and Hydroxyapatite Surface-grafted with L-lactic Acid Oligomer for Bone Repair. *Acta Biomater.* **2009**, *5* (7), 2680−2692.
(44) Tsai, W. B.; Chen, R. P. Y.; Wei, K. L.; Chen, Y. R.; Liao, T. Y.; Liu, H. L.; Lai, J. Y. Polyelectrolyte Multilayer Films Functionalized with Peptides for Promoting Osteoblast Functions. *Acta Biomater.* **2009**, *5* (9), 3467−3477.
(45) Cui, H. T.; Wang, Y.; Cui, L. G.; Zhang, P. B.; Wang, X. H.; Wei, Y.; Chen, X. S. In Vitro Studies on Regulation of Osteogenic Activities by Electrical Stimulus on Biodegradable Electroactive Polyelectrolyte Multilayers. *Biomacromolecules* **2014**, *15* (8), 3146−3157.
(46) Bayram, C.; Demirbilek, M.; Caliskan, N.; Demirbilek, M. E.; Denkbcs, E. B. Osteoblast Activity on Anodized Titania Nanotubes: Effect of Simulated Body Fluid Soaking Time. *J. Biomed. Nanotechnol.* **2012**, *8* (3), 482−490.
(47) Costa, D. O.; Prowse, P. D. H.; Chrones, T.; Sims, S. M.; Hamilton, D. W.; Rizkalla, A. S.; Dixon, S. J. The Differential Regulation of Osteoblast and Osteoclast Activity by Surface Topography of Hydroxyapatite Coatings. *Biomaterials* **2013**, *34* (30), 7215−7226.
(48) Chien, H. W.; Tsai, W. B. Fabrication of Tunable Micropatterned Substrates for Cell Patterning via Microcontact Printing of Polydopamine with Poly(ethylene imine)-grafted Copolymers. *Acta Biomater.* **2012**, *8* (10), 3678−3686.
(49) Nguyen, H.; Qian, J. J.; Bhatnagar, R. S.; Li, S. Enhanced Cell Attachment and Osteoblastic Activity by P-15 Peptide-coated Matrix in Hydrogels. *Biochem. Biophys. Res. Commun.* **2003**, *311* (1), 179−186.
(50) Sugiura, F.; Kitoh, H.; Ishiguro, N. Osteogenic Potential of Rat Mesenchymal Stem Cells After Several Passages. *Biochem. Biophys. Res. Commun.* **2004**, *316* (1), 233−9.
(51) Sa, M. A.; Ribeiro, H. J.; Valverde, T. M.; Sousa, B. R.; Martins-Junior, P. A.; Mendes, R. M.; Ladeira, L. O.; Resende, R. R.; Kitten, G. T.; Ferreira, A. J. Single-walled Carbon Nanotubes Functionalized with Sodium Hyaluronate Enhance Bone Mineralization. *Braz. J. Med. Biol. Res.* **2016**, *49* (2), e4888.
(52) Wu, C. T.; Zhou, Y. H.; Xu, M. C.; Han, P. P.; Chen, L.; Chang, J.; Xiao, Y. Copper-containing Mesoporous Bioactive Glass Scaffolds with Multifunctional Properties of Angiogenesis Capacity, Osteostimulation and Antibacterial Activity. *Biomaterials* **2013**, *34* (2), 422−433.
(53) Hoang, Q. Q.; Sicheri, F.; Howard, A. J.; Yang, D. S. C. Bone Recognition Mechanism of Porcine Osteocalcin from Crystal Structure. *Nature* **2003**, *425* (6961), 977−980.
(54) Prgeeth Pandula, P. K. C.; Samaranayake, L. P.; Jin, L. J.; Zhang, C. F. Human Umbilical Vein Endothelial Cells Synergize Osteo/Odontogenic Differentiation of Periodontal Ligament Stem Cells in 3D Cell Sheets. *J. Periodontal Res.* **2014**, *49* (3), 299−306.
(55) Wang, Z. L.; Wang, Y.; Zhang, P. B.; Chen, X. S. Methylsulfonylmethane-loaded Electrospun Poly(lactide-co-glycolide) Mats for Cartilage Tissue Engineering. *RSC Adv.* **2015**, *5* (117), 96725−96732.
(56) Shih, Y. R. V.; Hwang, Y.; Phadke, A.; Kang, H.; Hwang, N. S.; Caro, E. J.; Nguyen, S.; Siu, M.; Theodorakis, E. A.; Gianneschi, N. C.; Vecchio, K. S.; Chien, S.; Lee, O. K.; Varghese, S. Calcium Phosphate-bearing Matrices Induce Osteogenic Differentiation of Stem Cells through Adenosine Signaling. *Proc. Natl. Acad. Sci. U. S. A.* **2014**, *111* (3), 990−995.

DOI: 10.1021/acsami.6b08733
ACS Appl. Mater. Interfaces 2016, 8, 26559−26569